Multiplex immunofluorescence of spatial distribution of infiltrating T cells in different regions of hepatic lobules during liver transplantation rejection

Shipeng Li
Capital Medical University Affiliated Beijing Friendship Hospital
Guangpeng Zhou
Capital Medical University Affiliated Beijing Friendship Hospital
Jie Sun
Capital Medical University Affiliated Beijing Friendship Hospital
Bin Cui
Capital Medical University Affiliated Beijing Friendship Hospital
Haiming Zhang
Capital Medical University Affiliated Beijing Friendship Hospital
Lin Wei
Capital Medical University Affiliated Beijing Friendship Hospital
Liying Sun
Capital Medical University Affiliated Beijing Friendship Hospital
Zhijun Zhu (zhu-zhijun@outlook.com)
Capital Medical University Affiliated Beijing Friendship Hospital https://orcid.org/0000-0001-7031-2083

Research Article

Keywords: spatial distribution, infiltrating T cells, hepatic lobule regions, liver transplantation rejection, multiplex immunofluorescence

Posted Date: May 13th, 2021

DOI: https://doi.org/10.21203/rs.3.rs-508924/v1

Abstract

It is still unclear whether there are differences in the types and functional status of immune cells in different areas of the liver lobules after liver transplantation rejection. The composition of infiltrating T cells in liver allografts during liver transplantation rejection is unclear and difficult to visualize on the same biopsy slide. We used multiplex immunofluorescence assays to study the spatial distribution of various types of infiltrating T cells in different areas of the liver lobules after liver transplantation. In the same area of the hepatic lobules, the percentage of CD4 + T cells, CD8 + T cells and regulatory T cells (Tregs) in the acute rejection group was higher than that in the nonacute rejection and normal groups. Within all three groups, the percentage of CD4 + T cells, CD8 + T cells and Tregs from the periportal to perivenous zones was increased first and then decreased. The percentage of CD8 + T cells increased gradually from the periportal to perivenous zones, the percentage of CD8 + T cells in perivenous zone was higher than in the transitional and periportal zones in the rejection group. In conclusion, the percentage of CD8 + T cells in different regions of liver lobules is closely related to rejection level after liver transplantation. Acute liver transplantation rejection may occur when the percentage of CD8 + T cells in the perivenous zone increases. Although the percentage of regional CD4 + T could not reflect the rejection level, but the number of CD4 + and CD8 + T cells in different regions was closely related to the rejection level.

Introduction

Rejection is a major obstacle to the long-term survival of liver grafts and the prognosis of patients after liver transplantation[1,2]. Rejection includes cell-mediated cell rejection and humoral antibody mediated immune response[3]. In recent years, it has been proved that the changes of T cell subsets are different in transplant rejection. $CD4^+$ T cells can stimulate T cell clonal expansion and differentiation by recognizing allogeneic antigen and secreting interleukin (IL)-2, and induction of acute rejection by activating $CD8^+$ cytotoxic T cells[4]. T helper (Th)17 cells are immune cells that mainly secrete IL-17A, IL-17F and other cytokines, and mediate the inflammatory response[5]. It has been showed that T regulatory cells (Tregs) play an important role in inhibiting transplantation immune rejection and inducing immune tolerance[6]. The proportion of $CD4^+$ T cells, $CD8^+$ T cells and Th17 in peripheral blood of patients with acute rejection is increased, but the proportion of Tregs is increased in peripheral blood of patients without acute rejection[7]. At the same time, $CD4^+$ T cells, $CD8^+$ T cells, Th17 and Tregs in liver tissue also change accordingly.

To date, the exact phenotype of these immune cells has not been specified. However, different phenotypic and molecular studies have found that the composition of the infiltrating lymphocytes may be important. The liver consists of about 1 million hepatic lobules, and blood flows from the peripheral portal area to the central vein[8]. There are gradient changes in nutrition, oxygen concentration, hormones and other aspects in the hepatocyte plate of the hepatic lobule, thus forming different metabolic functional areas[9]. The hepatic lobules are divided into three regions according to their different metabolic functions: perivenous, transitional and periportal zones[8,9]. Halpern divided the porto-central lobule axis into nine layers and developed a probabilistic inference algorithm to calculate the likelihood of each cell belonging to any of these layers based on the expression of our panel of landmark genes[10]. The functional status of the corresponding non-hepatic parenchymal cells (endothelial cells, immune cells, etc.) may be different due to the different partition of the hepatic lobules.

Previous studies have found that Kupffer cells are enriched near periportal regions, with those closest to portal triads having distinct phenotypic properties[11]. However, the distribution of diverse resident immune cell types, the cellular and molecular mechanisms underlying the spatial organization of the liver immune system, and the functional consequences of asymmetric immune cell localization remain to be clarified. Kupffer cells are enriched in periportal regions and there are quantitative data detailing this patterning, with $MHCII^{hi}$ or $MHCII^{int}$ Kupffer cells showing a similar distance to the central vein[12]. These data reveal that the hepatic lobules contain a spatially polarized immune system ‘immune zonation’. However, there are no reports about the spatial distribution of infiltrating T cells and the changes in immune microenvironment in different areas of hepatic lobules during liver transplantation rejection. Due to the complexity of the structure of the hepatic lobules, the gene expression pattern of the spatial axis from the central vein to the portal zone is different, and its function also change gradually. Especially in the traditional hepatic lobule transitional zone, many important genes are expressed. Curiously, There is a question as to whether there are differences in the types and functional status of immune cells in different regions of hepatic lobules. In response to this question, we studied the infiltration and distribution of T cells in different regions of hepatic lobules, and the spatial distribution of T cells in different regions of hepatic lobules under conditions of acute and non-acute rejection after liver transplantation.

Previous studies have used immunohistochemical or immunofluorescence techniques to detect changes in CD4, CD8 and other indicators in grafts[13,14], but these techniques can only show a certain type of T cell distribution by one or two indicators. Here, we present a direct method that generated readouts for a comprehensive panel of biomarkers from liver biopsy from liver transplantation patients. Multiplex immunofluorescence staining can simultaneously label multi-cellular markers to observe various cell types and their functional status and interactions. It reveals details of the spatial localization of immune cells in different tissues, and gives a clear understanding of the immune microenvironment of organs and tissues[15]. Our research indicated that the infiltrated immune cells had spatial specificity and some exciting phenomena were found after liver transplantation. The distribution of $CD8^+$ T cells in different regions of hepatic lobules is closely related to rejection level after liver transplantation. Acute rejection of liver transplantation may occur when the percentage of $CD8^+$ T cells in perivenous zone increases. Although the percentage of regional $CD4^+$ T cells could not reflect the level of rejection, the number of $CD4^+$ T cells and $CD8^+$ T cells in different regions was closely related to the rejection level.

Materials And Methods

Patients and clinical data collection

Patients who underwent liver transplantation at Liver Transplantation Center, Beijing Friendship Hospital, Capital Medical University between January 2017 and July 2020 were included. Recipients' demographic, medical, transplantation, and follow-up data were collected (Table 1). Medical data comprised etiology of liver disease and laboratory data. Data related to transplantation were ABO blood group, donor sex and age, graft-type, operation time, and warm ischemic time. Laboratory data included trough concentration of tacrolimus and liver function tests such as albumin, aspartate aminotransferase (AST), alanine aminotransferase (ALT), and total bilirubin (TB). All liver grafts were voluntarily donated after cardiac death or by living donors, and all donations were approved by the Ethics Committee of Beijing Friendship Hospital, Capital Medical University.

Table 1
Baseline characteristic of liver transplantation recipients

Baseline characteristic	N1	N2	N3	R1	R2	R3	R4	NR1	NR2	NR3	NR4
Recipient											
Gender	female	male	female	female	male	female	male	female	male	female	female
Age (yr)	27	25	24	0.58	0.58	60	14	0.67	45	23	45
ABO	O	O	B	A	B	O	O	B	O	A	O
AST (U/L)	12.3	11.4	23.6	141.7	86.1	267.4	27.7	26.7	28.9	14.7	29.5
ALT (U/L	7	11	13	118	50	181	20	17	23	5	18
Albumin (g/L)	45.3	42.4	45.8	34.7	40.1	27.9	43.3	44.5	41.8	40.3	41.4
Total bilirubin (μmol/L)	5.54	12.35	11.54	34.53	7.95	92.69	11.11	21.59	18.46	6.72	11.41
HBV-positive	NO	NO	NO	NO	NO	YES	NO	NO	YES	NO	YES
HCV-positive	NO	NO	NO	NO	NO	NO	NO	NO	NO	NO	NO
Etiology	-	-	-	Liver failure	Biliary atresia	Liver cirrhosis	Hepatoblastoma	Biliary atresia	hepatocellular carcinoma	Hyperoxaluria	Liver cirrhosis
Donor organ type	-	-	-	living donor	living donor	DCD	DCD	living donor	DCD	DCD	DCD
RAI	0	0	0	5	7	5	5	1	2	1	1
Donor											
Gender	-	-	-	female	female	male	male	female	male	male	male
Age(yr)	-	-	-	26	25	35	27	25	39	42	34
ABO	-	-	-	A	B	O	O	B	O	A	O
Cold ischemic time (h)	-	-	-	57min	52min	142min	750min	52min	652min	520min	730min
Warm ischemic time (min)	-	-	-	4min	3min	8min	11min	3min	9min	3min	10min

Group management of liver transplantation patients

All liver transplantation patients were divided into the acute rejection and non-acute rejection groups according to the Banff schema for grading liver allograft acute rejection[16], and a normal group was set up. The total score of rejection activity index (RAI) was 9. The patients with a score less than 3 were classified as non-acute rejection, and 3–9 as acute rejection.

Liver histology

Liver biopsies were performed using the Menghini method under deep sedation with propofol[17]. Biopsies were performed by two experienced examiners with a 17-gauge needle. The specimen length was ≥ 2 cm. Normal liver tissues were obtained from living donors. The liver tissues were fixed in 4% mediosilicic isotonic formaldehyde for 24 h, dehydrated and embedded in paraffin. Four-micrometer-thick sections were cut from each paraffin embedded tissue and stained with hematoxylin and eosin (HE) to evaluate the pathological changes in the liver.

Immunocytochemistry

Immunocytochemistry staining was used to detect protein expression and distribution after microwave treatment. Following incubation in 3% H_2O_2 for 10 min, antibodies against CD4 (Abcam, Cambridge, MA, USA), CD8 (Abcam, Cambridge, MA, USA), IL-17 (Abcam, Cambridge, MA, USA) and FOXP3 (Abcam, Cambridge, MA, USA) were added and incubated at 4°C for 12h. The specimens were incubated with secondary antibodies at 37°C for 1 h, followed by diaminobenzidine staining.

Multiplex immunofluorescence assays [18]

Tissue multiplex immunofluorescent staining was performed using the Opal Polaris 5 color IHC staining kit (Akoya Biosciences). Briefly, tissue sections of 4-μm thick formalin-fixed, paraffin-embedded (FFPE) were baked for 2 h at 60°C before staining. Slides were rehydrated with a series of graded ethanol to deionized water. Antigen retrieval was performed at pH 6 for 20 min at 95°C. Slides were serially stained with the following antibodies: anti-CD4, -CD8, -IL-17 and -FOXP3. Anti-mouse / rabbit horseradish peroxidase (Cell Signaling Technology, Danvers, MA, USA) was used as the primary antibody. TSA-conjugated fluorophores (PerkinElmer) were used to visualize each biomarker: Opal 690 (IL-17), Opal 620 (FoxP3), Opal 570 (CD4) and Opal 520 (CD8), incubation time per primary antibody was 1 h. Subsequently, anti-rabbit/mouse Polymeric Horseradish Peroxidase (Opal IHC Detection Kit, Akoya Biosciences) was applied as a secondary label with an incubation time of 10 min. Antibody signal was visualized using the corresponding Opal Fluorophore (Akoya Biosciences) by incubating the slides for 10 min. Slides were mounted with anti-fade mounting medium (P36965, Life Technologies) and stored at 4°C before imaging. Image acquisition was performed using the Vectra Polaris multispectral imaging platform (Akoya Biosciences), whole slide image was scanned and 3–5 representative regions of interest were chosen by the pathologist at 200× resolution as multispectral images.

Hepatic lobule zone

The hepatic lobules are divided into three regions: perivenous, transitional and periportal zones, as previously described[8].

Statistical analysis

The data were expressed as mean ± standard deviation. Differences among groups were analyzed by one-way analysis of variance and Newman-Keuls test. SPSS version 22.0 was used for these analyses. A P value < 0.05 was considered as statistically significant.

Results

Pathological changes in liver

The histopathological features in acute rejection consisted of three major components of the lesion: inflammation of the portal tracts, bile duct damage, and endotheliitis. The portal tract showed a pleomorphic infiltrate of lymphocytes, neutrophils, and plasma cells. Considerable balloon like degeneration, cholestasis, necrosis, phlebitis and fibrosis were observed in the acute rejection group as compared with the normal group. Compared with acute rejection group, he staining showed that the infiltration of immune cells in portal area and hepatic lobule was significantly reduced in non-rejection group, bile duct injury and endothelial injury were rare, and hepatocyte edema and necrosis were reduced (Fig. 1A).

Expression and distribution of CD4, CD8, IL-17 and FOXP3 in liver tissues

Expression and distribution of CD4, CD8, IL-17 and FOXP3 were detected by immunohistochemistry (Fig. 1B). CD4 was mainly expressed in the membrane and cytoplasm of sinusoidal endothelial cells and lymphocytes. In normal liver tissue, CD4 was mainly expressed in liver sinusoidal endothelial cells, while $CD4^+$ T cells were few in number. In the acute rejection group, there were more infiltrating immune cells and $CD4^+$ T cells, but fewer $CD4^+$ liver sinusoidal endothelial cells. The infiltrating immune cells and $CD4^+$ T cells in the non-acute rejection group were significantly reduced, while the number of $CD4^+$ liver sinusoidal endothelial cells was increased. The expression and distribution of CD8 T cells were similar to those of CD4 + T cells. In normal liver tissue, there were few $CD8^+$ T cells, mainly concentrated in the portal area, and fewer infiltrated the hepatic lobules. $CD8^+$ T cells increased significantly in the acute rejection group. Compared with the acute rejection group, $CD8^+$ T cells decreased significantly in the non-acute rejection group. IL-17 was mainly expressed in hepatocytes, endothelial cells and immune cells cytoplasm. Compared with the normal and non-acute rejection groups, the expression of IL-17 in lymphocytes was higher in the acute rejection group. FOXP3 was mainly expressed in nucleus and immune cells. $FOXP3^+$ T cells were almost not found in normal liver tissue. There were significantly more $FOXP3^+$ T cells in the acute rejection than non-acute rejection group.

Multiplex immunofluorescence to measure dynamic changes in infiltrating T cells in liver acute rejection

To visualize changes in the composition of the immune infiltrate in liver acute rejection, we performed multiplexed immunofluorescence staining for CD4, CD8, IL-17 and FOXP3 (Fig. 2A). We calculated the proportion of various types of T cells in each slice (N% = number of certain T cells / total number of cells in each slice×100%), and compared the differences in T cells in each group. This revealed an increase of infiltrating $CD4^+$ T cells in the acute rejection and non-acute rejection groups as compared with the normal group, The proportion of $CD4^+$ T cells was highest in the acute rejection group, and the difference was statistically significant (Fig. 2B, $P < 0.001$). The number of infiltrating $CD8^+$ T cells was highly variable among patients in the normal group (Fig. 2C, $P < 0.001$). We also detected numbers of infiltrating FOXP3 + regulatory T cells ($CD4^+FOXP3^+$ T and $CD8^+FOXP3^+$ T cells) in the liver. It was difficult to observe $CD4^+FOXP3^+$ T (Tregs) and $CD8^+$FOXP3 + T cells in the normal and non-acute rejection groups, but the proportion of Tregs and $CD8^+$ $FOXP3^+$ T cells in the acute rejection group was the highest, and the difference was significant (Fig. 2D and 2E, $P < 0.001$). We also counted the number of $CD4^+IL\text{-}17^+$ T (Th17) and $CD8^+IL\text{-}17^+$ T cells, and the proportion of Th17 cells in the acute rejection group was the highest, and the difference was significant (Fig. 2F, $P < 0.001$). The number of CD8 + IL-17 + T cells in liver tissue was low, although the proportion was still the highest in the acute rejection group (Fig. 2G, $P < 0.001$). The above results showed that the proportion of $CD4^+$ T cells, $CD8^+$ T cells, Tregs, and Th17 increased in acute rejection after liver transplantation, and these cells were involved in the formation of acute rejection or immune tolerance after liver transplantation. When the rejection level decreased or there was no rejection, these types of T cells decreased or even disappeared.

Distribution of infiltrating T cells in hepatic lobule and portal area

Due to the difference in the structure of hepatic lobule and portal area (Fig. 3A and 3B), the distribution of inflammatory cell infiltration is also different. We observed the difference in T cell distribution in hepatic lobules and portal area by multiple staining technique, and summarized the characteristics of T cell spatial distribution in the liver under different immune states of liver transplantation (Fig. 3C). In the normal group, there were few infiltrating T cells in the hepatic lobules, and a small number of $CD8^+$ T cells, $CD4^+$ T cells, $CD4^+$ $FOXP3^+$ T cells (Tregs), $CD4^+$ $IL\text{-}17^+$ T cells (Th17). In the acute rejection group, the number of infiltrating T cells was significantly increased, including $CD8^+$ T cells, while the number of $CD8^+$ T cells was higher than that of CD4 + T cells. The number of infiltrating T lymphocyte in the non-acute rejection group was lower than that in the acute rejection group; $CD8^+$ T cells and $CD4^+$ T cells were seen, but Tregs and Th17 could rarely be observed. In the normal group, infiltrating T cells could be seen in the portal area, mainly $CD8^+$ T cells and CD4 + T cells. A small number of Th17 were also seen, but there were no Tregs. In the acute rejection group, infiltrating T cells were seen in the portal area, with a large number of $CD8^+$ T cells and $CD4^+$ T cells, and Tregs and Th17 were also observed. The number of infiltrating T cells in non-acute rejection group was lower than that in acute rejection group, $CD8^+$ T cells and $CD4^+$ T cells were seen, but there were fewer Tregs and Th17 (Fig. 3C). The above results showed that the distribution of infiltrating T cells was different in the hepatic lobules and portal area. The infiltrating T cells mainly concentrated in the portal area, and a few infiltrated the hepatic lobules.

Distribution of T cell infiltration in different areas of hepatic lobules

The hepatic lobule is divided into the perivenous, transitional and the periportal zones (Fig. 4A and 4B). The percentage of $CD4^+$ T cells, CD8 + T cells and Tregs in each region was statistically analyzed (n% = the number of T cells / total number of cells in the each zone×100%), and then the differences were compared in the different rejection states of liver transplantation. As showed in Fig. 4D, we compared the spatial distribution of periportal zone $CD4^+$ T cells, $CD8^+$ T cells and Tregs in the normal, acute rejection and non-acute rejection groups. Multiplex immunofluorescence staining showed that the percentage of Tregs in the acute rejection group was significantly higher than that of other two groups ($P < 0.001$). The percentage of $CD4^+$ T cells and $CD8^+$ T cells was higher than in the normal group ($P < 0.01$). The percentage of $CD4^+$ T cells and $CD8^+$ T cells in the non-rejection group was higher than that of the normal group ($P < 0.05$). The percentage of $CD4^+$ T cells in non-rejection group was significantly lower than that in acute rejection group, but significantly higher than that in normal group ($P < 0.05$). In the transitional zone, the percentage of $CD4^+$ T cells and Tregs in the acute rejection group was higher than that of the other two groups ($P < 0.01$), the percentage of $CD8^+$ T cells was higher than that of the normal group ($P < 0.05$); the percentage of $CD4^+$ T cells in the non-rejection group was significantly higher than in the non-rejection group ($P < 0.05$). The percentage of $CD4^+$ T cells, $CD8^+$ T cells and Tregs was lower than in the acute rejection group, but higher than in the normal group ($P < 0.05$). At the same time, the proportion of $CD4^+$ T cells, $CD8^+$ T cells and Tregs in perivenous zone in the acute rejection group was higher than that of the other two groups ($P < 0.05$). The percentage of $CD4^+$ T cells, $CD8^+$ T cells in the non-rejection group was lower in the acute rejection group, but higher than in the normal group ($P < 0.05$).

We observed the difference in T cell spatial distribution in different regions of liver tissue in the same group (Fig. 4E). In the normal group, the percentage of $CD4^+$ T cells and Tregs in different regions was different, but not statistically ($P > 0.05$). The percentage of transitional zone $CD4^+$ T cells was significantly higher than in the other two regions in the normal group ($P < 0.05$). Similarly, the percentage of $CD4^+$ T cells from the periportal to perivenous zones was different in the acute rejection group, but not statistically ($P > 0.05$). Interestingly, the percentage of $CD8^+$ T cells from the periportal to perivenous zones increased gradually, the percentage of CD8 + T cells in perivenous zone was higher than in other two zones ($P < 0.05$). The percentage of transitional zone Tregs was higher than that of perivenus zone ($P < 0.05$). The percentage of $CD4^+$ T cells and $CD8^+$ T cells from the periportal to perivenous zones was different in the non-acute rejection group, but not significantly ($P > 0.05$). The percentage of Tregs in the transitional zone in the non-rejection group was significantly higher than in the other two regions ($P < 0.05$).

Discussion

T cells play an important role in the rejection of allogeneic liver transplantation[19], and participate in the recognition of transplantation antigens, immune regulation, cell dissolving effect and other immune responses[20,21]. In order to study the phenotype and quantity of T cells in different rejection levels after liver transplantation, the changes of $CD4^+$ T cells, $CD8^+$ T cells, Tregs and Th17 in peripheral blood were detected by flow cytometry or immunohistochemistry. After liver transplantation, the levels of blood $CD4^+$ T cells peaked in the acute rejection group and was significantly higher than that of the non-acute rejection group[22]. Tregs and Th17 are known to be involved in the alloreactive responses in organ transplantation. Wang et al[23] investigated whether the circulating Tregs/Th17 ratio is associated with acute allograft rejection in liver transplantation. The frequency of circulating Tregs was significantly decreased, whereas the frequency of circulating Th17 cells was significantly increased in acute rejection. Tregs/Th17 ratio had a negative correlation with liver damage indices and the score of rejection activity index after liver transplantation.

When immune rejection occurs, a large number of T cells infiltrate the graft, such as CD4 and CD8 subsets, which increases with the aggravation of rejection[24]. The most important histological changes of acute rejection are mixed inflammatory cell infiltration of the confluence area[25]. Krukemeyer et al[26] found that more B lymphocytes and plasma cells migrated to the liver in patients with rejection than in non-rejection patients through liver tissue studies. But these experimental techniques have some limitations. The exact composition of leukocyte infiltration during liver allograft rejection is difficult to comprehend and visualize on the same biopsy slide. With the development of science and technology, multiplex immunofluorescence assays has been favored by researchers.

Multiplexed imaging platforms to simultaneously detect multiple epitopes in the same tissue section have emerged in recent years as powerful tools to study the immune context of organs and tissues[27]. Multiplex immunofluorescence assays can improve the understanding of the tissue microenvironment, new therapeutic targets, prognostic and predictive biomarkers, and translational studies[28]. Until now, this new technology has mainly been used in oncology to better characterize immune cell infiltration in tumors in situ[29–31]. Previous studies have used immunohistochemical or immunofluorescence techniques to

detect the changes in $CD4^+$ T cells, $CD8^+$ T cells, Th17, Tregs and other indicators in grafts. However, using serial tissue sections makes the cellular interplay and the precise location of the cells difficult to analyze. We present multiplex immunofluorescence assays that generated readouts for a comprehensive panel of biomarkers from liver biopsies from liver transplantation patients. Our findings revealed increased infiltration of $CD4^+$ T and $CD8^+$ T cells in the acute rejection and non-acute rejection groups as compared with the normal group. The proportion of $CD4^+$ and $CD8^+$ T cells in the acute rejection group was the highest. There were also some interesting note was that it was difficult to observe Tregs in the normal and non-acute rejection groups, but the proportion of Tregs and Th17 was the highest in the acute rejection group. The above results showed that the proportion of $CD4^+$ T cells, $CD8^+$ T cells, Tregs and Th17 increased during acute rejection after liver transplantation, and these cells were involved in the development of acute rejection or immune tolerance after liver transplantation. Calvani et al[32]detected simultaneously NK cells, macrophages, and T cells to determine their intra- or extravascular localization using multiplex immunofluorescence assays, demonstrating the feasibility and utility of multiplex immunofluorescence imaging to study and better understand the kidney allograft rejection process. The above results show that different types of lymphocytes infiltrate different immune states after organ transplantation. The mechanism through which different immune cells participate in rejection or immune tolerance is different.

When acute rejection occurs, interlobular bile duct and vascular endothelial cells are the primary targets of immune attack[33]. Many immune cells infiltrate the mixed portal area and hepatic lobules, and cause venous endothelial inflammation and bile duct inflammation[34]. Similarly, our immunofluorescence staining results showed that infiltrating T cells could be seen in the portal area, including a large number of $CD8^+$ T cells, $CD4^+$ T cells, Tregs and Th17 in the acute rejection group. The number of infiltrating T lymphocytes in the non-acute rejection group was less than that in the acute rejection group. We found a novel phenomenon: more lymphocytes infiltrated hepatic lobules under higher levels of the rejection, but the number of CD4 + sinusoidal endothelial cells decreased significantly. Previous studies have showed that tissue-resident immune cells are important for organ homeostasis and defense, and the epithelium may contribute to these functions directly or by crosstalk with immune cells[35]. The mechanism of interaction between T cells and sinusoidal endothelial cells in acute rejection of liver transplantation needs further study.

The above results showed that the distribution of infiltrating T cells was different in the hepatic lobules and portal area. Due to the complexity of hepatic lobule structure, it can be divided into three regions according to different metabolic functions. The gene expression patterns of the spatial axis from the central vein to portal area are different, at the same time, its function is gradual[10]. Because liver lobules contain a spatially polarized immune system "immune zonation", the types and numbers of immune cells infiltrating hepatic lobules are different in different disease states[12]. Kupffer cells can localize infiltrating neutrophils to the periportal regions of the lobule, limiting damage to cells that reside around the central vein[36]. It remains unclear whether there are differences in the types and functional status of immune cells in different regions of hepatic lobules under different rejection conditions after liver transplantation. We used multiple immunofluorescence staining to study the infiltration and distribution of T cells in different areas of hepatic lobules, and the spatial distribution of various types of T cells in different areas of hepatic lobules under acute rejection and non-acute rejection after liver transplantation. The results showed that the infiltrated immune cells had some spatial specificity and some exciting phenomena were found after liver transplantation. In the same area of the hepatic lobule, the percentages of $CD4^+$ T cells, $CD8^+$ T cells and Tregs in the rejection group was higher than that in the other two groups, which indicated that the percentage of these T cells increased in each area of the hepatic lobule when rejection occurred. Within three group, percentage of $CD4^+$ T cells, $CD8^+$ T cells and Tregs from periportal zone to perivenous zone were initially increased and then decreased. Interestingly, the percentage of $CD8^+$ T cells from the periportal to perivenous zones increased gradually, the percentage of $CD8^+$ T cells in the perivenous zone was higher than that in the other two zones in the rejection group. Renal allograft biopsies showing c-aABMR show a predominance of infiltrating $CD8^+$ T cells, and increased numbers of interstitial $FOXP3^+$ T cells are associated with inferior allograft survival[37]. Similarly, the distribution of $CD8^+$ T cells in different regions of hepatic lobules may be closely related to rejection level after liver transplantation.

There were some limitations in our study, such as the small number of clinical samples, the difficulty in obtaining liver biopsy specimens, and the incomplete structure of hepatic lobules in liver biopsy tissue. These deficiencies may have led to instability of the results. Therefore, this study needs to be further improved to find other novel results. In conclusion, we believe that the percentage of $CD8^+$ T cells in different regions of hepatic lobules is closely related to rejection level after liver transplantation. We observed an important heterogeneity in the global composition of the inflammatory burden during liver allograft rejection. Acute rejection of liver transplantation may occur when the percentage of $CD8^+$ T cells in perivenous zone increase, and Tregs increases reactively. The number and proportion of $CD8^+$ T cells increased gradually from the periportal to perivenous zones under different rejection levels. Although the percentage of regional CD4 + T did not reflect the rejection level, the number of $CD4^+$ and $CD8^+$ T cells in different regions was closely related to the rejection level.

Declarations

Ethics approval and consent to participate

The study protocol was approved by the ethics committee of Beijing Friendship Hospital, Capital Medical University, Beijing, China

Consent for publication

All authors have reviewed the manuscript and have given consent for publication.

Availability of data and materials

All data generated or analyzed during this study are available in this article.

Competing interests

The authors declare no conflicts of interest in this work.

Funding

This work was supported by the National Natural Science Foundation of China (No. 81970562).

Authors' contributions

Shipeng Li and Zhijun Zhu contributed to the research design. Guangpeng Zhou, Jie Sun and Bin Cui collected the clinical data; Shipeng Li and Jie Sun performed multiplex immunofluorescence staining and immunocytochemistry. Haiming Zhang, Lin Wei and Liying Sun contributed to the data management and statistical analyses. Shipeng Li and Zhijun Zhu wrote the manuscript.

Acknowledgements

The authors would like to thank the Key Laboratory of Transplantation immunity of Beijing for their technical support.

References

1. Taner, T. 2017. Liver transplantation: Rejection and tolerance. *Liver Transpl* 23 (S1): S85–S88.
2. Wei, Q., K. Wang, and Z. He, et al. 2018. Acute Liver Allograft Rejection After Living Donor Liver Transplantation: Risk Factors and Patient Survival. *Am J Med Sci* 356 (1): 23–29.
3. Duizendstra, A. A., M. Doukas, and M. Betjes, et al. HLA matching and rabbit antithymocyte globulin as induction therapy to avoid multiple forms of rejection after a third liver transplantation. *Clin Res Hepatol Gastroenterol*. 2020:101539.
4. Chen, X., J. Zheng, and J. Cai, et al. 2017. The cytoskeleton protein beta-actin may mediate T cell apoptosis during acute rejection reaction after liver transplantation in a rat model. *Am J Transl Res* 9 (11): 4888–4901.
5. Xie, X. J., Y. F. Ye, and L. Zhou, et al. 2010. Th17 promotes acute rejection following liver transplantation in rats. *J Zhejiang Univ Sci B* 11 (11): 819–827.
6. Le Moine, A. 2021. What are the effects of everolimus and basiliximab on Tregs regulation and tolerance after liver transplantation? *Clin Res Hepatol Gastroenterol* 45 (5): 101591.
7. Haarer, J., P. Riquelme, and P. Hoffmann, et al. 2016. Early Enrichment and Restitution of the Peripheral Blood Tregs Pool Is Associated With Rejection-Free Stable Immunosuppression After Liver Transplantation. *Transplantation* 100 (7): e39–e40.
8. Steiner, P. E., and H. L. Ratcliffe. 1968. The hepatic lobules of suidae, tayassuidae, and hippopotamidae. *Anat Rec* 160 (3): 531–538.
9. Chikamori, K., T. Araki, and M. Yamada. 1985. Pattern analysis of the heterogeneous distribution of succinate dehydrogenase in single rat hepatic lobules. *Cell Mol Biol* 31 (3): 217–222.
10. Halpern, K. B., R. Shenhav, and O. Matcovitch-Natan, et al. 2017. Single-cell spatial reconstruction reveals global division of labour in the mammalian liver. *Nature* 542 (7641): 352–356.
11. Sleyster, E. C., and D. L. Knook. 1982. Relation between localization and function of rat liver Kupffer cells. *Lab Invest* 47 (5): 484–490.
12. Gola, A., M. G. Dorrington, and E. Speranza, et al. 2021. Commensal-driven immune zonation of the liver promotes host defence. *Nature* 589 (7840): 131–136.
13. Okamura, A., T. Matsushita, and A. Komuro, et al. 2020. Adipose-derived stromal/stem cells successfully attenuate the fibrosis of scleroderma mouse models. *Int J Rheum Dis* 23 (2): 216–225.
14. Chen, Z., J. Liu, and D. Xu. 2021. [Oncolytic adenovirus expressing CCL19 enhances immunity against gastric cancer in mice]. *Xi Bao Yu Fen Zi Mian Yi Xue Za Zhi* 37 (2): 119–124.
15. Mauldin, I. S., A. Mahmutovic, S. J. Young, and C. J. Slingluff. 2021. Multiplex Immunofluorescence Histology for Immune Cell Infiltrates in Melanoma-Associated Tertiary Lymphoid Structures. *Methods Mol Biol* 2265: 573–587.
16. Demetris, A. J., C. Bellamy, and S. G. Hubscher, et al. 2016. 2016 Comprehensive Update of the Banff Working Group on Liver Allograft Pathology: Introduction of Antibody-Mediated Rejection. *Am J Transplant* 16 (10): 2816–2835.
17. Rasmussen, S. N., H. H. Holm, J. K. Kristensen, and H. Barlebo. 1972. Ultrasonically-guided liver biopsy. *Br Med J* 2 (5812): 500–502.
18. Canadas, I., R. Thummalapalli, and J. W. Kim, et al. 2018. Tumor innate immunity primed by specific interferon-stimulated endogenous retroviruses. *Nat Med* 24 (8): 1143–1150.
19. Crosbie, O. M., S. Norris, J. E. Hegarty, and C. O'Farrelly. 1998. T lymphocyte subsets and activation status in patients following liver transplantation. *Immunol Invest* 27 (4–5): 237–241.
20. Natsuda, K., S. Eguchi, and M. Takatsuki, et al. 2016. CD4 T lymphocyte counts in patients undergoing splenectomy during living donor liver transplantation. *Transpl Immunol* 34: 50–53.
21. Jiang, Z., Y. Chen, and X. Feng, et al. 2013. Recipient cytotoxic T lymphocyte antigen 4 + 49 single-nucleotide polymorphism is not associated with acute rejection after liver transplantation in Chinese population. *Int J Med Sci* 10 (3): 250–254.
22. Dong, J. Y., H. Yin, and R. D. Li, et al. 2011. The relationship between adenosine triphosphate within CD4(+) T cells and acute rejection after liver transplantation. *Clin Transplant* 25 (3): E292–E296.

23. Wang, Y., M. Zhang, and Z. W. Liu, et al. 2014. The ratio of circulating regulatory T cells (Tregss)/Th17 cells is associated with acute allograft rejection in liver transplantation. *Plos One* 9 (11): e112135.
24. Kamada, N., H. S. Davies, D. Wight, L. Culank, and B. Roser. 1983. Liver transplantation in the rat. Biochemical and histological evidence of complete tolerance induction in non-rejector strains. *Transplantation* 35 (4): 304–311.
25. Qian, S., L. Lu, and Y. Li, et al. Apoptosis of graft-infiltrating cytotoxic T cells: a mechanism underlying "split tolerance" in mouse liver transplantation. *Transplant Proc*. 1997;29(1–2):1168-9.
26. Krukemeyer, M. G., J. Moeller, and L. Morawietz, et al. 2004. Description of B lymphocytes and plasma cells, complement, and chemokines/receptors in acute liver allograft rejection. *Transplantation* 78 (1): 65–70.
27. Lee, C. W., Y. J. Ren, and M. Marella, et al. 2020. Multiplex immunofluorescence staining and image analysis assay for diffuse large B cell lymphoma. *J Immunol Methods* 478: 112714.
28. Francisco-Cruz, A., E. R. Parra, M. T. Tetzlaff, and I. I. Wistuba. 2020. Multiplex Immunofluorescence Assays. *Methods Mol Biol* 2055: 467–495.
29. Viratham, P. A., S. G. Craig, and V. Bingham, et al. 2020. A robust multiplex immunofluorescence and digital pathology workflow for the characterisation of the tumour immune microenvironment. *Mol Oncol* 14 (10): 2384–2402.
30. Parra, E. R., N. Uraoka, and M. Jiang, et al. 2017. Validation of multiplex immunofluorescence panels using multispectral microscopy for immune-profiling of formalin-fixed and paraffin-embedded human tumor tissues. *Sci Rep* 7 (1): 13380.
31. Parra, E. R., J. Zhai, and A. Tamegnon, et al. 2021. Identification of distinct immune landscapes using an automated nine-color multiplex immunofluorescence staining panel and image analysis in paraffin tumor tissues. *Sci Rep* 11 (1): 4530.
32. Calvani, J., M. Terada, and C. Lesaffre, et al. 2020. In situ multiplex immunofluorescence analysis of the inflammatory burden in kidney allograft rejection: A new tool to characterize the alloimmune response. *Am J Transplant* 20 (4): 942–953.
33. Porter, K. A. 1969. Pathology of liver transplantation. *Transplant Rev* 2: 129–170.
34. Lefkowitch, J. H. 2002. Diagnostic issues in liver transplantation pathology. *Clin Liver Dis* 6 (2): 555–570. ix.
35. Stewart, B. J., J. R. Ferdinand, and M. D. Young, et al. 2019. Spatiotemporal immune zonation of the human kidney. *Science* 365 (6460): 1461–1466.
36. Halpern, K. B., R. Shenhav, and H. Massalha, et al. 2018. Paired-cell sequencing enables spatial gene expression mapping of liver endothelial cells. *Nat Biotechnol* 36 (10): 962–970.
37. Sablik, K. A., E. S. Jordanova, N. Pocorni, G. M. Clahsen-van, and M. Betjes. 2019. Immune Cell Infiltrate in Chronic-Active Antibody-Mediated Rejection. *Front Immunol* 10: 3106.

Figures

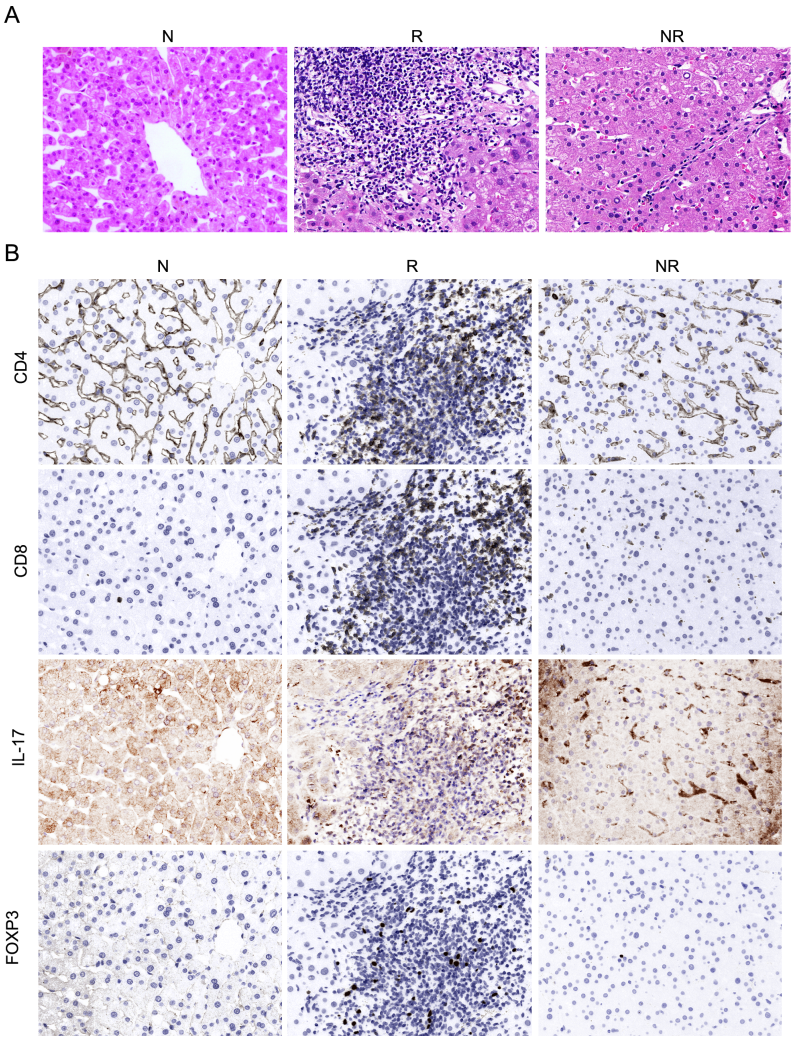

Figure 1

Expression of T cell related markers in liver tissues (A) HE staining was used to observe the pathological changes of liver tissue in each group (×200). (B) Expressions of CD4, CD8, IL-17 and FOXP3 in liver tissue in each group were detected with use of immunohistochemistry (×200).

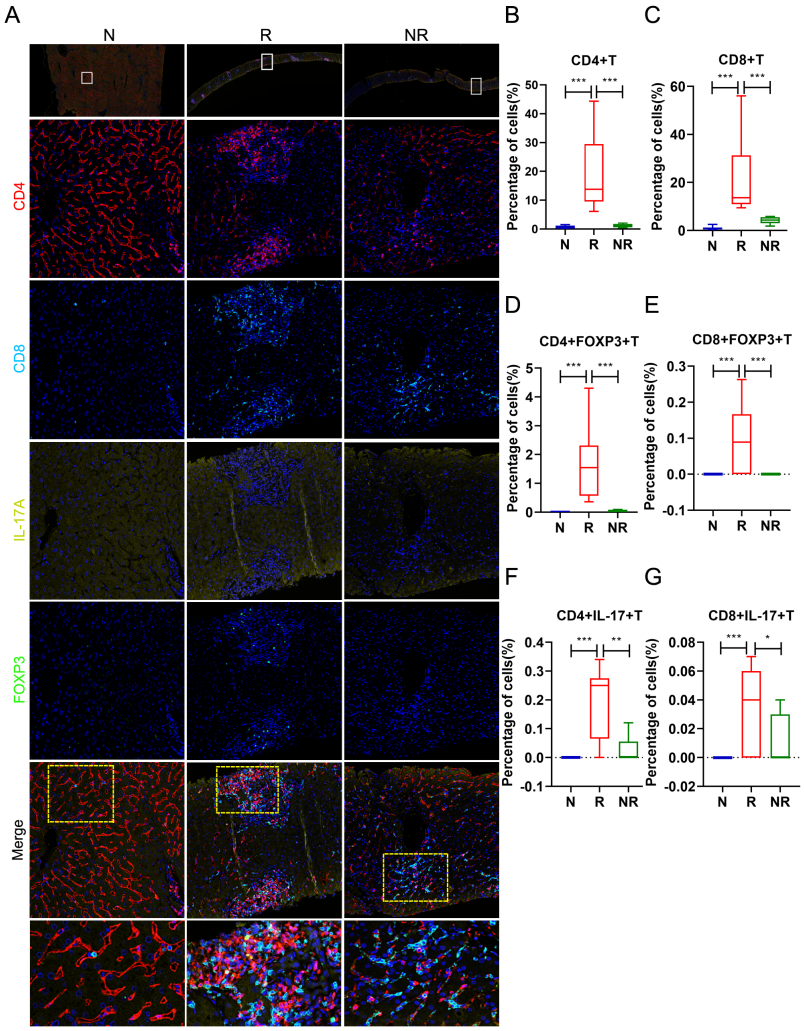

Figure 2

Increased T-cell infiltration related to rejection after liver transplantation (A) Multiplexed immunofluorescence staining of immune cell marker panel (CD4-red, CD8-light blue, IL-17-yellow, FOXP3-green) and DAPI (blue) of liver tissue in each group (×200). (B) The percentage of CD4+T, CD8+T, CD4+FOXP3+T, CD8+FOXP3+T, CD4+IL-17+T and CD8+ IL-17+T cells in liver tissue in each group. *P<0.05, **P<0.01, ***P<0.001 compared with R group.

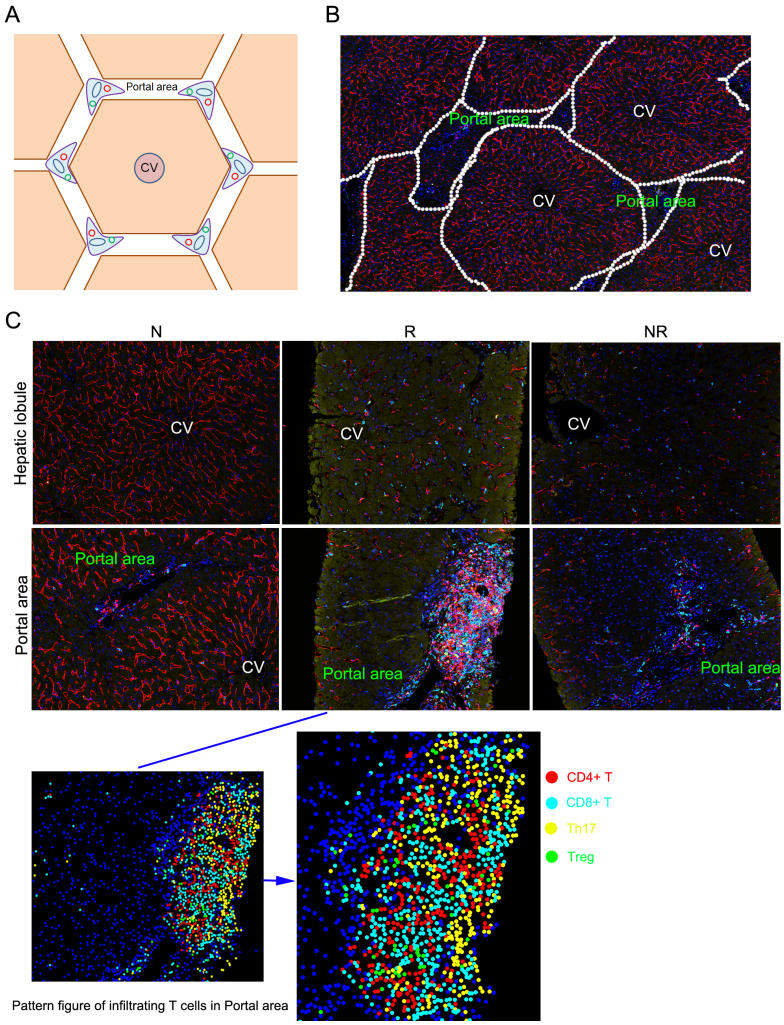

Figure 3

Distribution of infiltrating T cells in hepatic lobule and portal area (A) Pattern of hepatic lobules and portal area.(B) Schematic diagram of boundary between hepatic lobules and portal area.(C) Multiplexed immunofuorescence staining of immune cell marker panel (CD4-red, CD8-light blue, IL-17-yellow, FOXP3-green) and DAPI (blue) in hepatic lobules and portal area in each group (×200).

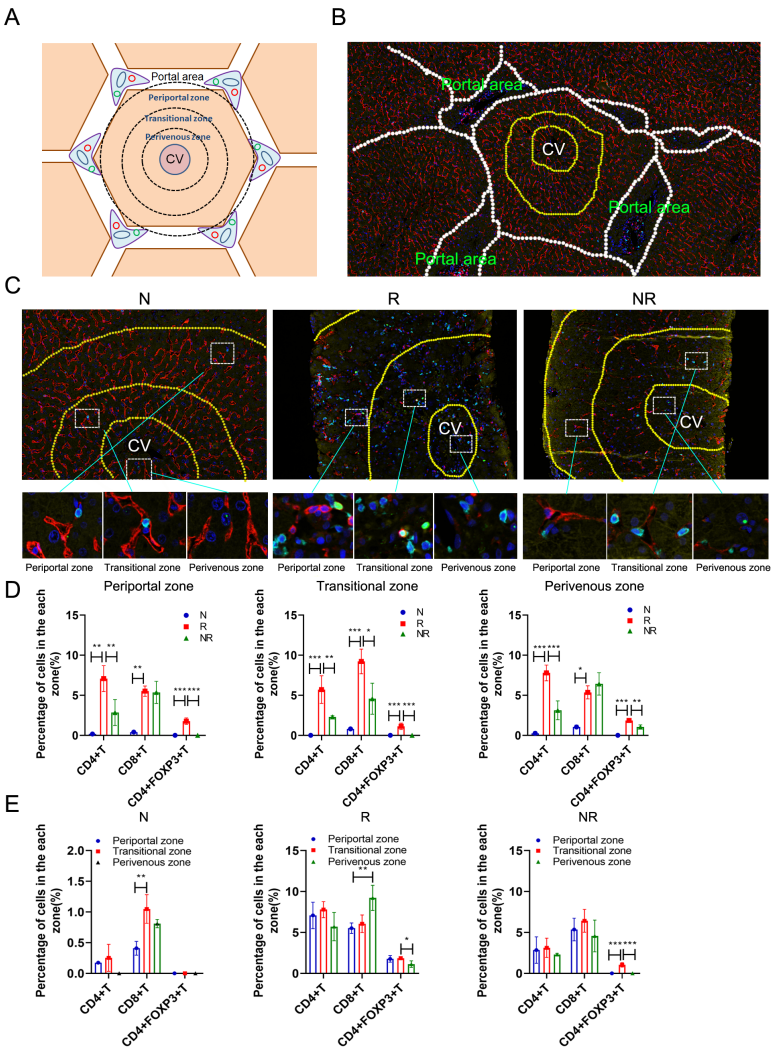

Figure 4

Distribution of infiltrating T cells in different regions of hepatic lobule (A) Pattern of hepatic lobular division.(B) Schematic diagram of boundary among hepatic lobular divisions.(C) Multiplexed immunofluorescence staining of immune cell marker panel (CD4-red, CD8-light blue, IL-17-yellow, FOXP3-green) and DAPI (blue) in perivenous, transitional and periportal zones (×200). (D) Within the same area (periportal zone, transitional zone or perivenous zone), the percentage of CD4+T, CD8+T and CD4+FOXP3+ T cells in N, R and NR groups (×200). *P<0.05, **P<0.01, ***P<0.001 compared with R group. (E) Within the same group (N, R or NR group), the percentage of CD4+T, CD8+T and CD4+FOXP3+ T cells in periportal zone, transitional zone or perivenous zone (×200). *P<0.05, ***P<0.001 compared with transitional zone.